

On the Turbulent Flow Structures over a Short Finite Cylinder: Numerical Investigation

Khodayar Javadi

Sharif University of Technology, Aerospace Department
Tehran, Iran
Kjavadi@sharif.edu

Farzad Kinai

Aerospace Research Institute
Tehran, Iran
farzad_kiani1364@yahoo.com

Abstract -This paper, describes the physics of a turbulent flow over a short finite circular cylinder. For this purpose, a free end finite circular cylinder with low aspect ratio, $L/D=2$, which is perpendicularly mounted over a surface is considered. The Reynolds number based on cylinder diameter is 20000. A uniform flow at upstream of the cylinder is considered as the inlet boundary condition. Since most of the flow features in this problem are unsteady, therefore, large eddy simulation (LES) is used to resolve detail unsteady turbulent pattern and time averaged mean flow features. At the top free end of the cylinder in addition to a big recirculation region, tip vortices are clearly observed which are in agreement with previous investigation. The instantaneous horseshoe vortex near the ground is found to be unsteady and changed shape over time. There is a downwash flow above the free end into the near wake region which occurs at an approximately constant angle with respect to the plane normal to the streamwise direction.

Keywords: Finite cylinder, Separated turbulent flow, Horse shoe vortices, Wake region.

1. Introduction

In recent century, circular cylinders in cross-flow is one of the considerable practical and fundamental fluid-mechanics interest (Strelets 2001; Frederich, Wassen, and Thiele 2008; Zhang and Guo 2006; S.-S. Chen 1987; Palau-Salvador et al. 2010; KAWAMURA et al. 1984; Igbalajobi et al. 2012; Park and Lee 2002; Fröhlich and Rodi 2004; Krajnovic 2011; Liu, So, and Cui 2005; Rostamy et al. 2012; Williamson 1996; Pattenden, Turnock, and Zhang 2005; Agui and Andreopoulos 1992; Pattenden et al. 2007; Roh and Park 2003; Afgan et al. 2007; Heseltine 2011; Iungo, Pii, and Buresti 2012; Zdravkovich 2003; Afgan, Moulinec, and Laurence 2006; OKAMOTO and YAGITA 1973; Luo 1993). The flow around finite circular cylinders, which one end standing in a flat-plate boundary layer and other end is free, have extremely application in engineering design such as buildings, stacks, cooling towers, offshore platforms, power lines, bridge supports, heat exchangers, nuclear cooling towers, gas tanks, space rockets on launching pads and chimneys design.

Quite complex three-dimensional flow field develops, when a long circular cylinder is standing in the boundary layer of the flat plate (see figure 1). As shown in figure 1 (Agui and Andreopoulos 1992) horseshoe vortex forms at the cylinder-wall junction. These horseshoe vortex can cause material elimination at the cylinder-wall junction, which can lead to the failure of the pier, bridge, and pylon (Heseltine 2011; Pattenden, Turnock, and Zhang 2005). Another major complexity of the flow structure occurs at the free end of the cylinder due to flow interact with the cylinder leading edge at the free end (Krajnovic 2011).

Although in the laminar flow, fluid moves regular in a classified layer which molecules and the fluid viscosity are the factors of motion, however, there are significant irregularities in the formation of lines in the turbulent flow. In this case, instead of the molecules, eddies transfer the kinetic energy and

momentum.

This flow field structure extremely depends on several non-dimensional characteristic parameters. The Reynolds number (based on the cylinder diameter the height-to-diameter ratio (l/d) and the relative boundary layer thickness of the approach flow, (δ/l), are the important parameters in the finite-height case (Rostamy et al. 2012; Krajnovic 2011; Frederich, Wassen, and Thiele 2008).

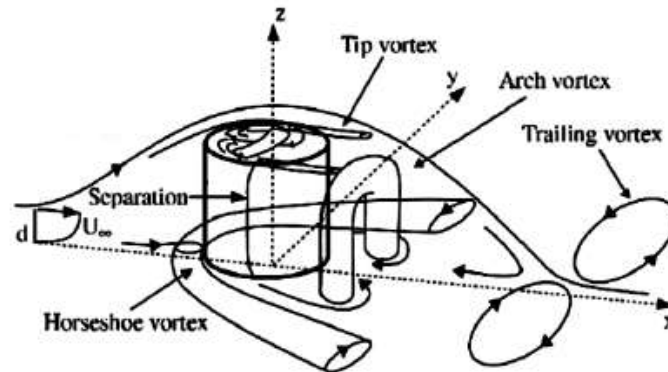


Fig. 1. Sketch of flow structure around the finite circular cylinder (Agui and Andreopoulos 1992).

To obtain complete physical understanding of the wake behavior, especially very close to the cylinder and similar geometry (Rostamy et al. 2012; Afgan et al. 2007; Strelets 2001), further studies are needed due to considering the complexity of the flow field around the finite circular cylinder. Previous studies (Baker 1980; Zdravkovich 2003; Williamson 1996; Williamson 1985; S.-S. Chen 1987) have examined two-dimensional flow around a circular cylinder. However, this assumption neglected the three-dimensional, free end, and wall-junction effects. Some of 3D effects are not truly captured without 3D assumption such as alternating vortex shedding causing large fluctuating pressure forces that can lead to noise, vibration, or even structural failure when the vortex shedding frequency coincides with the bodies' own natural frequency.

(OKAMOTO and YAGITA 1973) measured the surface pressure coefficients at $Re=1.3 \times 10^4$ for cylinders of aspect ratios 1–15 immersed in a uniform flow. They also found in their study that the impression of the free end on the near wake flow was limited to the three diameters from the top of the cylinder. (Roh and Park 2003) studied flow structures at free end surface region of a finite circular cylinder at two different $L/D = 1.25$ and 4.25 and varying Reynolds numbers (5.92×10^3 and 1.48×10^5).

(Iungo, Pii, and Buresti 2012) investigated the wake structure generated from a finite height circular cylinder placed vertically on a plane. They found that the mean drag coefficient is roughly invariant by varying the Reynolds number in a range between 6×10^4 and 11×10^4 . (Igbalajobi et al. 2012) investigated experimentally the influence of a wake-mounted splitter plate on the flow around a surface-mounted of a finite height circular cylinder where the Reynolds number was 7.4×10^4 . They studied mean drag force coefficient and the vortex shedding frequency for different $L/D = 9, 7, 5,$ and 3 and different lengths of splitter (1 to 7) and found that the splitter plate be a less effective drag-reduction device for finite circular cylinders.

Recent developments in computer power causes the CFD tools and the numerical simulations become one of the most accurate and reliable method to investigate the complex phenomena. In this case, a selection of turbulence model is important to predict accurately the characteristics of the flow.

(Liu, So, and Cui 2005) simulated the flow past the finite circular cylinder with $L/D=10$ at Reynolds numbers varying from 100 to 200. They used the lattice Boltzmann method and found that in this Reynolds range, the wake behavior and flow-induced forces are greatly affected by Re . Also the Reynolds effects on the necklace and trailing vortices with the variation of the Strouhal number, and the mean and root mean square drag and lift coefficients along the span are studied.

The large eddy simulation (LES) method, which models the small scale eddies and calculates the

large scale eddies needs finer grid than the RANS approach. However, the DNS model that small-scale eddies should calculate requires more computational grid compare to the LES methods. The LES model is a viable alternative to the exact solution, near the wall LES accuracy is less than the RANS models, but its increases in high Reynolds number (Viswanathan 2006; Said 2007).

Maybe the first large eddy simulation of the finite cylinder flow was by (Fröhlich and Rodi 2004), they have simulated a flow where $L/D = 2.5$ at $Re = 4.3 \times 10^4$. (Zhang and Guo 2006) used the fluent 6.2 software with the LES approach and investigate the highly complex interaction between turbulent flow and deep-sea marina. They studied three different heights of circular cylinder by fixed diameter with a range of Reynolds number $1.0 \times 10^4 \sim 1.0 \times 10^5$. They also carried out wake properties, complex separated flow structures.

The flow around a free end circular cylinder was simulated using the LES and DES at Reynolds number based on a diameter of 200000 by (Pattenden et al. 2007). They made a comparison between the abilities of the two models and their own experimental results that captured flow features observed in particle image velocimetry (PIV).

(Frederich, Wassen, and Thiele 2008) made the LES and DES for short cylinder $L/D=2$ and compare with different experiment and numerical to show the dependence of results to L/D , they also show that the LES results in an attached laminar boundary layer better than the DES model. Other studies show that the difference height-to-diameter ratio (L/D) causes various flow structures at near wake and separation regions (Frederich, Wassen, and Thiele 2008; Krajnovic 2011; Pattenden et al. 2007; Zhang and Guo 2006; Afgan, Moulinec, and Laurence 2006). Therefore, flow structure around circular cylinder is highly dependent on L/D .

Palau-Salvador et al. (Palau-Salvador et al. 2010), made the LES of their own experimental cases with $L/D = 2.5$ at $Re = 4.3 \times 10^4$ and $L/D = 5$ at $Re = 2.2 \times 10^4$. They compared the results for the velocities and turbulence stresses between their experimental observations and the LES simulation. They showed that their simulation for a short wall mounted cylinder predicts the flow in rather good agreement with the experimental data, although they presented the recirculation zone behind the cylinder and showed that it was slightly over predicted.

(Afgan, Moulinec, and Laurence 2006) presented the LES of the flows studied by (Park and Lee 2002) where $L/D=6$ and 10 at $Re = 2.0 \times 10^4$. Also the most recent numerical simulation has been done by (Krajnovic 2011) who either made turbulent numerical simulation of the LES model of (Park and Lee 2002) experiments at $L/D=6$ and showed marvelous vortex physics at near the weak, free end, and wall-junction. However, in present work flow structures around finite short circular cylinder with $l/d = 2$ and $Re_d = 2.0 \times 10^4$, have been investigated in details.

Some of the mentioned investigations above are summarized with the most important parameters in table 1 and compared with the present work.

Table 1. Investigations used for comparison

Authors	Year	Exp./Num.	L/D		
(OKAMOTO and YAGITA 1973)	1973	-	1-15	1.3×10^4	
(Park and Lee 2002)	2002	Exp.	6	2.0×10^4	-
(Roh and Park 2003)	2003	Exp.	1.25, 4.25	$5.92 \times 10^3, 1.48 \times 10^3$	-
(Fröhlich and Rodi 2004)	2004	Num.	2.5	4.3×10^4	LES
(Liu, So, and Cui 2005)	2005	Num.	10	100,200	Lattice Boltzmann
(Zhang and Guo 2006)	2006	Num.	3.083, 3.167	$1.0 \times 10^4 \sim 1.0 \times 10^5$	LEs
(Afgan et al. 2007)	2007	Num.	6, 10	2.0×10^4	LES
(Pattenden et al. 2007)	2007	Exp./Num.	1	2.0×10^3	LES/DES
(Frederich, Wassen, and Thiele 2008)	2008	Num.	2	2.0×10^3	LES/DES
(Palau-Salvador et al. 2010)	2010	Exp./Num.	2.5,5	$4.3 \times 10^4, 2.2 \times 10^4$	LES
(Krajnovic 2011)	2011	Num.	6	2.0×10^4	LES
(Iungo, Pii, and Buresti 2012)	2012	Exp.	2	$6.0 \times 10^4, 11 \times 10^4$	-
(Igbalajobi et al. 2012)	2012	Exp.	9,7,5,3	7.4×10^4	-
Present work	2013	Num.	2	2.0×10^4	LES

Although different researchers have studied this problem, less numerically and much more

experimentally, there are many unanswered questions on this problem yet to be answered such as detail of the flow near the free end of the cylinder. Also there are different theories on the mean flow structures and tip vortex formation. In this regard, the aim of this work is to do investigations on this problem to help understanding and if possible exploring some unanswered open question. To this end large eddy simulation technique is used to resolve instantaneous flow features and mean time averaged structures of the flow over a short finite free end cylinder with $L/D=2$.

2. Problem Definition and Computational Domain

The flow structure around short finite circular cylinder standing in a flat-plate boundary layer is predicted using numerical turbulence approaches Large-Eddy Simulation (LES). The geometry and flow condition used in the present study are design due to this structure application in flow control which will illustrate in future. Investigations are carried out using a finite circular cylinder with a diameter of $D = 0.1\text{m}$ and a length-to-diameter ratio of $l/d = 2$ and the free stream inlet velocity $U_0=20\text{m/s}$, which gives based on the diameter a Reynolds number of approximately 2×10^4 . In the present study the geometry and computational domain of the problem are shown in figure 2. Figure 3 shows the 3D structured grid (total element = 7504000) used to predict the flow field around the finite circular cylinder. Y^+ ranges on the cylinder and ground is between 0.237 and 16.800 for the LES turbulence model (Afgan et al. 2007; Krajnovic 2011) with time step 0.00005 that causes minimum courant number (CFL) 0.37 (Krajnovic 2011). To achieve stable conditions, simulations have been done for 14000 time steps to pass the inlet flow through the entire computational domain for 5 times. The present results are obtained by statistical time averaging of the last 5400 time steps.

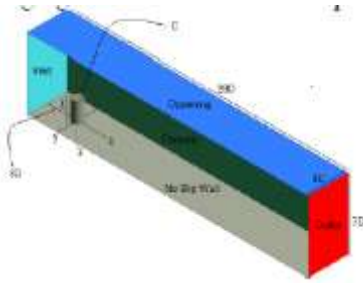


Fig. 2. Sketch of the investigated configuration

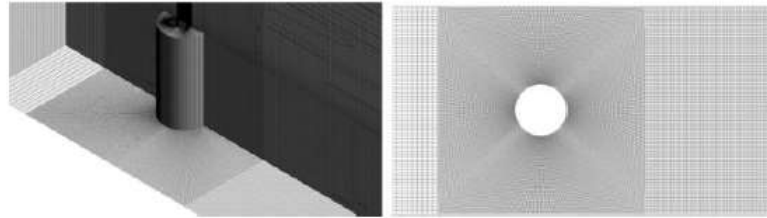


Fig. 3. Computational grid over the finite circular cylinder

2. 1. Boundary Conditions

Uniform velocity profile, constant in time, was thus used as the inlet boundary condition. The convective boundary condition was used at the outlet boundary. The ceiling was treated as slip surfaces using an opening boundary condition that can be specified with a Relative Pressure value. The value is interpreted as relative total pressure for inflow and relative static pressure for outflow. No-slip boundary conditions were used on the surface of the body and instantaneous wall functions were applied on finite cylinder wall and floor channel. Periodic boundary conditions were used on the lateral surfaces, where conservative interface flux happens at these boundaries. These periodic boundary conditions have been used due to the structure application in flow control which will illustrate in future presentation.

3. Governing Equations

The governing equations for this problem are conservation of mass and momentum for the case of unsteady incompressible 3D flow as follow:

Where the extra term, sub-grid scale stress, is the results of small eddy effects and define as bellow:

$$\frac{\partial \bar{U}_i}{\partial x_i} = 0 \quad (1)$$

$$\frac{\partial \bar{U}_i}{\partial t} + \frac{\partial}{\partial x_j} (\bar{U}_i \bar{U}_j) = -\frac{1}{\rho} \frac{\partial P}{\partial x_i} + \frac{\partial}{\partial x_j} \left[\nu \left(\frac{\partial \bar{U}_i}{\partial x_j} + \frac{\partial \bar{U}_j}{\partial x_i} \right) \right] - \frac{1}{\rho} \frac{\partial \tau_{ij}}{\partial x_j} \quad (2)$$

Where the extra term τ_{ij} , sub-grid scale stress, is the results of small eddy effects and define as bellow:

$$\tau_{ij} = \overline{U_i U_j} - \overline{U_i} \overline{U_j} \quad (3)$$

In this approach, the large scale eddies are simulated directly by the main grid and the discretization scheme and effect of the small eddies are modeled with the sub-grid scale (SGS) as:

$$-\left[\tau_{ij} - \frac{\delta_{ij}}{3} \tau_{kk}\right] = 2v_{sgs} \overline{S_{ij}} \quad , \quad \overline{S_{ij}} = \frac{1}{2} \left(\frac{\partial \overline{U_i}}{\partial x_j} + \frac{\partial \overline{U_j}}{\partial x_i} \right) \quad (4)$$

$$v_{sgs} = (C_w \Delta)^2 \frac{(S_{ij}^d S_{ij}^d)^{3/2}}{(\overline{S_{ij}} \overline{S_{ij}})^{5/2} + (S_{ij}^d S_{ij}^d)^{5/4}} \quad (5)$$

Where $C_w = 0.5$ is constant and the local grid size, Δ , is calculated by $\Delta = (\text{Vol})^{1/3}$. Also the velocity gradient traceless quadratic symmetry tensor, S_{ij}^d , can be written using the strain rate and the vorticity tensors as:

$$S_{ij}^d = \overline{S_{ik}} \overline{S_{kj}} + \overline{\Omega_{ik}} \overline{\Omega_{kj}} - \frac{1}{3} \delta_{ij} (\overline{S_{mn}} \overline{S_{mn}} - \overline{\Omega_{mn}} \overline{\Omega_{mn}}) \quad (7)$$

Where the vorticity tensor $\overline{\Omega_{ij}}$ is defined as:

$$\overline{\Omega_{ij}} = \frac{1}{2} \left(\frac{\partial \overline{U_i}}{\partial x_j} - \frac{\partial \overline{U_j}}{\partial x_i} \right) \quad (8)$$

4. Results and Discussions

Passing flow over a free end finite cylinder is a highly complex flow field containing many unsteady structures such as unsteady wake region, tip vortexes, Karman-like vortex street, and to resolve these unsteady feature and explore the pattern of flow field as much as more realistic LES was used as turbulence approach to validate and to verify the obtained results in this work, pressure coefficient distribution around the cylinder was compared with available numerical and experimental data as shown in **Figure 4** the results shows good agreement between them. **Figure 5**, shows the length of the recirculation region at symmetry plane of the cylinder. As shown, there is a good agreement between our LES simulation and previous data. Also from **Figure 5**, it is clear that there is a downwash flow above the free end into the near wake region which occurs at an approximately constant angle with respect to the plane normal to the streamwise direction.

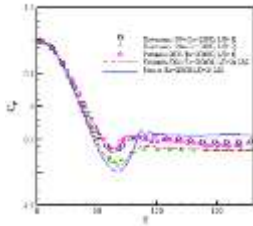


Fig. 4. Pressure coefficient on the cylinder shell at $z/D = -1$ of LES compared to experimental results by Kawamura et al. (1984) and Pattenen et al. (2005), numerical LES Frederich et al. (2008) and numerical simulations

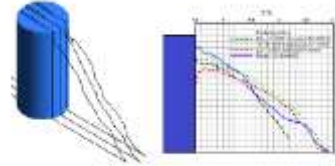


Fig. 5. Time-averaged recirculation region ($= 0$) in the symmetry plane of LES, $Re=20,000$ compared with experiments of Leder (2003, LDA-03, $Re=200,000$), Jensch et al. (2006, TR-PIV, $Re=200,000$) and numerical Frederich et al. (2008 LES, $Re=200,000$).

4. 1. Instantaneous Analysis

The highly complex phenomena, such as the unsteady separated bubble, the turbulent wake are shown **Figure 6** and the horseshoe vortex is shown **Figure 7**, these transition features were founded by (Agui and Andreopoulos 1992). (KAWAMURA et al. 1984) showed that height-to-diameter ratio and the relative boundary layer thickness influence the flow behaviour. the Kármán vortex shedding that exists behind infinite cylinders, as shown in **Figure 8**, is the results of the downwash flow from the top free end of the cylinder and the trailing vortices which are met in the near wake region, see Fig. **Figure 6** and **Figure 7**. The Kármán vortex shedding is dependent on the cylinder aspect ratio and it is available only for cylinders that have aspect ratio higher than critical value which was later found by other researchers and reported it is vary between $l/d=1$ to 7. The reason for the dependency of this phenomena to the critical aspect ratio values was found in the influence of the plane boundary layer (Luo 1993). The downwash, **Figure 6**, and **Figure 7** trailing vortices dominate the vortex shedding pattern, **Figure 8**, more details on this phenomenon is presented by (Pattenen, Turnock, and Zhang 2005).



Fig. 6: Unsteady separated flow at top of the cylinder and downwash wake region behind the cylinder.

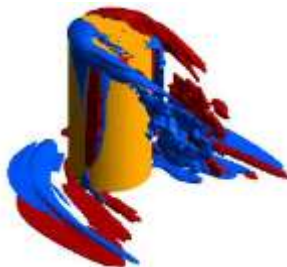


Fig. 7: Tip vortex at tip free

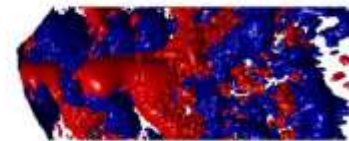


Fig. 8: unsteady Karman Vortex end and horseshoe vortices at the ground.

4. 2. Time Averaged Mean Features

Another major complexity of the flow structure occurs at the free end of the cylinder due to flow interact with the cylinder leading edge at the free end. As shown in **Figure 9**, the is separated from the leading edge of the cylinder and a big unsteady recirculating region is produced. Despite the relatively simple geometry, the flow structure near the free end of a circular cylinder is not well understood (Krajnovic 2011). There have been a number of measurements of the aerodynamic forces, surface pressures and wake periodicity; however, there have been few studies that have measured the wake velocity field downstream of the cylinder tip (Afgan et al. 2007). The tip vortices formation, as is illustrated in **Figure 9**, is the results of the interaction of the Kármán flow along the upper part of the cylinder and the flow over the free end which is in agreement with (Krajnovic 2011). Similar vortices are known to exit whenever a lifting surface, such as a wing, terminates in a fluid and usually have undesirable effects (Heseltine 2011). Furthermore, existence of some other vortices such as arch vortex,

Figure 10, and trailing vortices (see figure 1) enhances the complexity of these structures and causes the flow field around the finite circular cylinder becomes strongly turbulent, **Figure 6** and **Figure 11**, as reported by other researchers (Pattenden, Turnock, and Zhang 2005). Arc-shaped vortex, as shown in **Figure 10**, is one of the well-known structures generated by passing a moving fluid over a finite short cylinder. This phenomena has been addressed by many researcher (Agui and Andreopoulos 1992; Krajnovic 2011; Pattenden et al. 2007), previously. The arc-vortex has a symmetric topology in our simulation which is in agreement with previous studies as reported by (Krajnovic 2011), for low aspect ratio ($L/d=4$). However, by increasing the aspect ratio the shape of the vortex becomes more asymmetric rather than symmetric.

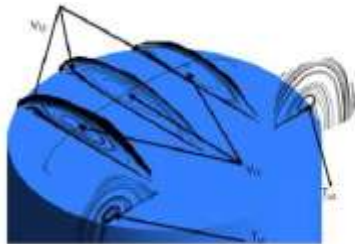


Fig. 9 Separated bubble and tip vortex formation at top free end



Fig. 10. Arc vortex behind the cylinder

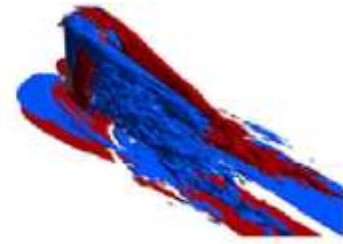


Fig. 11. Downwash flow and trailing edge vortices behind of the cylinder

5. Conclusion

The turbulent flow over a wall mounted short finite free end cylinder with $L/D=2$ was simulated using LES. At free end formation of unsteady tip vortex, trailing vortex, and recirculation bubble were observed. At the junction of the cylinder with wall the separated upstream-backflow creates the horse shoe vortex. Arc-shaped vortex which is one the phenomena addressed by many researchers, generated by passing a moving fluid over a finite short cylinder was captured in the present work. The results showed that for the $L/D=2$ this arc-shaped vortex has a symmetric topology. The Kármán vortex shedding behind infinite cylinder is formed due to combination of the downwash flow from the free end together the trailing vortices in the near wake region. The downwash and trailing vortices dominate the vortex shedding pattern at the wake region downstream of the cylinder. Also at the wake region, there is a downwash flow originate from top free end of the cylinder elongated into the near wake region. The angle of this downwash flow occurs at an approximately constant angle with respect to the plane normal to the streamwise direction.

References

- Afgan, Imran, Charles Moulinec, and Dominique Laurence. 2006. Large eddy simulation of flow over a vertically mounted finite cylinder on a flat plate. In *Conference on Modelling Fluid Flow (CMFF 2006). The 13th International Conference on Fluid Flow Technologies, Budapest, Hungary.*
- Afgan, Imran, Charles Moulinec, Robert Prosser, and Dominique Laurence. 2007. "Large eddy simulation of turbulent flow for wall mounted cantilever cylinders of aspect ratio 6 and 10." *International Journal of Heat and Fluid Flow* 28 (4): 561-574.
- Agui, J H, and J Andreopoulos. 1992. "Experimental investigation of a three-dimensional boundary layer flow in the vicinity of an upright wall mounted cylinder." *ASME Transactions Journal of Fluids Engineering* 114: 566-576.
- Baker, C J. 1980. "The turbulent horseshoe vortex." *Journal of Wind Engineering and Industrial Aerodynamics* 6 (1): 9-23.
- Chen, Ching Jen, and Shing-Yuh Jaw. 1998. *Fundamentals of turbulence modeling.* Taylor & Francis.
- Chen, Shoen-Sheng. 1987. "Flow-induced vibration of circular cylindrical structures." *Washington, DC, Hemisphere Publishing Corp., 1987, 487 p. Research supported by AEC, ERDA, and DOE.* 1.
- Frederich, O, E Wassen, and F Thiele. 2008. "Prediction of the Flow Around a Short Wall-Mounted

- Finite Cylinder using LES and DES1." *JNAIAM* 3 (3-4): 231-247.
- Fröhlich, Jochen, and Wolfgang Rodi. 2004. "LES of the flow around a circular cylinder of finite height." *International journal of heat and fluid flow* 25 (3): 537-548.
- Heseltine, Jonathan Lucas. 2011. "Flow around a circular cylinder with a free end."
- Igbalajobi, A, J F McClean, D Sumner, and D J Bergstrom. 2012. "The effect of a wake-mounted splitter plate on the flow around a surface-mounted finite-height circular cylinder." *Journal of Fluids and Structures*.
- Iungo, Giacomo Valerio, L M Pii, and G Buresti. 2012. "Experimental investigation on the aerodynamic loads and wake flow features of a low aspect-ratio circular cylinder." *Journal of Fluids and Structures* 28: 279-291.
- Jensch, M, M Brede, F Richter, and A Leder. 2006. "Verwendung des Time-Resolved Stereo-PIV Messsystems zur Ermittlung zeitaufgelöster Geschwindigkeitsfelder im Nachlauf eines Kreiszyinders." *Lasermethoden in der Strömungsmesstechnik-14. Fachtagung der GALA eV*: 31-39.
- KAWAMURA, Takao, Munehiko HIWADA, Toshiharu HIBINO, Ikuo MABUCHI, and Masaya KUMADA. 1984. "Flow around a finite circular cylinder on a flat plate (cylinder height greater than turbulent boundary layer thickness)." *Bulletin of the JSME* 27 (232): 2142-2151.
- Krajnovic, Sinisa. 2011. "Flow around a tall finite cylinder explored by large eddy simulation." *Journal of Fluid Mechanics* 676: 294-317.
- Leder, Alfred. 2003. 3D-flow structures behind truncated circular cylinders. In .
- Liu, Y, R M C So, and Z X Cui. 2005. "A finite cantilevered cylinder in a cross-flow." *Journal of fluids and structures* 20 (4): 589-609.
- Luo, S C. 1993. "Flow past a finite length circular cylinder."
- Nicoud, F, and F Ducros. 1999. "Subgrid-scale stress modelling based on the square of the velocity gradient tensor." *Flow, Turbulence and Combustion* 62 (3): 183-200.
- OKAMOTO, Tetsushi, and Miki YAGITA. 1973. "The experimental investigation on the flow past a circular cylinder of finite length placed normal to the plane surface in a uniform stream." *Bulletin of JSME* 16 (95): 805-814.
- Palau-Salvador, Guillermo, Thorsten Stoesser, Jochen Fröhlich, Michael Kappler, and Wolfgang Rodi. 2010. "Large eddy simulations and experiments of flow around finite-height cylinders." *Flow, turbulence and combustion* 84 (2): 239-275.
- Park, Cheol-Woo, and Sang-Joon Lee. 2002. "Flow structure around a finite circular cylinder embedded in various atmospheric boundary layers." *Fluid Dynamics Research* 30 (4): 197-215.
- Pattenden, R J, N W Bressloff, S R Turnock, and X Zhang. 2007. "Unsteady simulations of the flow around a short surface-mounted cylinder." *International journal for numerical methods in fluids* 53 (6): 895-914.
- Pattenden, R J, S R Turnock, and X Zhang. 2005. "Measurements of the flow over a low-aspect-ratio cylinder mounted on a ground plane." *Experiments in Fluids* 39 (1): 10-21.
- Richter, F. 2005. Experimentelle Untersuchungen zur Charakterisierung der Strömungs- und Turbulenzstrukturen im Nachlauf eines Kreiszyinders unter Berücksichtigung der Zentrifugalbeschleunigung. PhD thesis, University of Rostock, Germany.
- Roh, S, and S Park. 2003. "Vortical flow over the free end surface of a finite circular cylinder mounted on a flat plate." *Experiments in fluids* 34 (1): 63-67.
- Rostamy, N, D Sumner, D J Bergstrom, and J D Bugg. 2012. "Local flow field of a surface-mounted finite circular cylinder." *Journal of Fluids and Structures* 34: 105-122.
- Said, Abdel-Halim Saber Salem. 2007. Large Eddy Simulation of Shear-Free Interaction of Homogeneous Turbulence with a Flat-Plate Cascade. Virginia Polytechnic Institute and State University.
- Strelets, M. 2001. Detached eddy simulation of massively separated flows. In AIAA 2001-0879, 39th Aerospace Sciences Meeting and Exhibit, Reno, NV. doi:10.2514/6.2001-879.
- Viswanathan, Aron K. 2006. Detached Eddy Simulation of Turbulent Flow and Heat Transfer in Turbine Blade Internal Cooling Ducts. Virginia Polytechnic Institute and State University.
- Williamson, C H K. 1985. "Evolution of a single wake behind a pair of bluff bodies." *Journal of Fluid Mechanics* 159: 1-18. 1996. "Vortex dynamics in the cylinder wake." *Annual review of fluid*

mechanics 28 (1): 477-539.

Zdravkovich, Momchilo M. 2003. *Flow around Circular Cylinders: Volume 2: Applications*. Vol. 2. Oxford University Press.

Zhang, Jisheng, and Yakun Guo. 2006. Large eddy simulation of 3D turbulent flow around deep-sea marina structure. In *European Conference on Computational Fluid Dynamics*.